

## COMMUNICATION

[View Article Online](#)  
[View Journal](#) | [View Issue](#)

 Cite this: *J. Anal. At. Spectrom.*, 2014, 29, 2256  
[click for updates](#)

 Received 17th September 2014  
 Accepted 7th October 2014

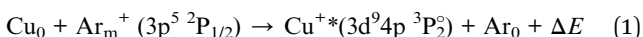
DOI: 10.1039/c4ja00309h

[www.rsc.org/jaas](http://www.rsc.org/jaas)

Transition rate diagrams of copper ions in argon and neon glow discharges are presented, using data from Cu II emission spectra. Based on the transition rate diagrams, several different collisional processes between ground state and metastable atoms and ions of copper and the discharge gas are proposed as probably significant for populating upper levels of the Cu II emission lines observed.

## 1. Introduction and experimental details

Studies of excitation and ionization of copper in glow discharge plasmas have been ongoing for many years, in connection with analytical applications of atomic spectroscopy, hollow cathode lamps, metal vapor ion lasers, magnetron sputtering for thin film deposition and in the diagnostics of astrophysical plasmas. A good introduction to the subject is provided in the works by Zhao and Horlick.<sup>1,2</sup> The key step to understanding the Cu II spectrum in argon glow discharges was made by Steers and Fielding in 1987 when they found out that the 224.700 nm line, by far the strongest Cu II emission line in a glow discharge in argon, is excited by asymmetric charge transfer between 3p<sup>5</sup> 2P<sub>1/2</sub> metastable argon ions and ground state copper atoms:<sup>3</sup>



In this equation and throughout the paper, the asterisk \* refers to an excited state of the respective species and the subscripts 0 and m mean the ground state and a metastable state, respectively. Steers *et al.* extended the work on Cu II

excitation to include a supplementary microwave discharge<sup>4,5</sup> and discharges in neon<sup>5,6</sup> and krypton.<sup>6</sup> In 1991, Wagatsuma and Hirokawa studied Cu II spectra in argon–helium glow discharges.<sup>7,8</sup> The computer modelling of glow discharge excitation of copper in studies by Bogaerts *et al.*<sup>9–11</sup> was a remarkable effort. The effects of hydrogen on Cu II spectra in argon and neon discharges were studied by Hodoroaba *et al.*<sup>12,13</sup> and Mushtaq *et al.*<sup>14</sup> Matrix effects in glow discharge emission spectroscopy related to the excitation of copper were studied by Weiss.<sup>15</sup> Classification of selective and non-selective excitation processes in argon–helium plasmas, involving also copper, was presented by Mushtaq *et al.*<sup>16</sup> The Cu II spectrum from a neon discharge is also discussed in a recent study by the same authors.<sup>17</sup>

It was shown very clearly that asymmetric charge transfer (ACT) reactions between copper atoms and ions of argon, neon and helium take place in glow discharges with these discharge gases and produce excited copper ions. ACT is a resonant process<sup>1–6</sup> and most studies listed above were therefore focused on Cu II lines with upper levels close to the ionization energy of the discharge gas and lines emitted as a result of cascade deexcitation of such levels. With the exception of the study of Steers and Leis,<sup>4</sup> the work of Rozsa *et al.*<sup>18</sup> and of Mezei *et al.*,<sup>19</sup> very little attention has been paid to Cu II levels with higher energies than the ionization energy of the discharge gas and the excitation/ionization processes involved. These higher levels are also excited, although to a much lesser degree. Recently, the formalism of transition rate diagrams (TR diagrams) was proposed by Weiss *et al.*,<sup>20,21</sup> which makes it possible to investigate quantitatively selective excitation processes in glow discharge spectra and thus identify individual reactions taking place. The present study is an attempt to describe systematically excitation processes in the Cu II spectrum in argon and neon glow discharges by the corresponding TR diagrams, with emphasis on Cu II levels with higher energies than the ionization energy of the discharge gas.

The spectral data referred to in this paper come largely from the vacuum-UV high resolution Fourier transform spectrometer

<sup>a</sup>LECO Instrumente Plzeň, spol. s r.o., Plaská 66, 323 25 Plzeň, Czech Republic. E-mail: weissz@leco.cz

<sup>b</sup>London Metropolitan University, 166–220 Holloway Road, London, N7 8DB, UK

<sup>c</sup>Blackett Laboratory, Imperial College London, Prince Consort Road, London, SW7 2AZ, UK

<sup>d</sup>Leibniz-Institut für Festkörper- und Werkstoffforschung Dresden, P.O.B. 27 01 16, D-01171 Dresden, Germany



(FTS)<sup>22</sup> at Imperial College London, used in conjunction with a free-standing Grimm-type source. Three wavelength ranges were selected by choosing appropriate free spectral ranges and suitable photomultiplier tube detectors and, where needed, optical filters. The combined wavelength range of these FTS measurements was from 151 to 630 nm. The resolution used was:  $0.035\text{ cm}^{-1}$  for the visible region ( $>365\text{ nm}$ );  $0.05\text{ cm}^{-1}$  for the intermediate region (250–365 nm), and  $0.07\text{ cm}^{-1}$  for the UV-VUV region (151–250 nm). This corresponds to a resolution of  $0.14\text{ pm}$  at  $200\text{ nm}$ . Radiometric calibration of the FTS spectra was performed using standard lamps, a tungsten-halogen lamp and a deuterium lamp, with known radiation characteristics, and by the branching ratio method.<sup>21</sup> The procedure will be described in more detail in a forthcoming paper on a new catalogue of glow discharge spectra. Spectral data from two CCD-based glow discharge spectrometers, the LECO GDS500<sup>15</sup> at the LECO European Technical Centre, Prague, and the Spectrum GDA650<sup>23</sup> at IFW Dresden were also used to give better sensitivity in some wavelength regions. All the measurements mentioned above were made using a Grimm-type glow discharge source<sup>20,21,23</sup> with a 4 mm internal anode diameter and a flat cathode (the sample investigated). A dc discharge was used, operating at  $700\text{ V}$  and  $20\text{ mA}$ , with the constant voltage-constant current stabilization and pure copper as the cathode. The pressure needed to maintain these conditions was  $805\text{ Pa}$  in argon and  $2010\text{ Pa}$  in neon as the discharge gas.

## 2. Results and discussion

The Cu II transition rate diagrams resulting from the observed Cu II spectra in argon and neon glow discharges are in Fig. 1 and 2. The concept of TR diagrams<sup>20,21</sup> can be described as follows: Intensity  $I_{ij}$  of an emission line associated with a radiative transition  $i \rightarrow j$  between an upper level  $i$  and a lower level  $j$  of an atom or ion can be expressed as:

$$I_{ij} = n_{i \rightarrow j} E_{ij} = n_{i \rightarrow j} \frac{hc}{\lambda_{ij}}$$

where  $\lambda_{ij}$  is the wavelength of this line,  $E_{ij}$  is the energy difference between the levels  $i$  and  $j$ ,  $n_{i \rightarrow j}$  is the rate of this transition, *i.e.*, the number of such transitions occurring per second. From this equation it follows that the rate  $n_{i \rightarrow j}$  is proportional to the product  $I_{ij} \lambda_{ij}$ . Transition rates associated with different emission lines can thus be evaluated from the observed spectrum, except for a common multiplicative constant. In this sense, the quantities referred to as transition rates are transition rates expressed in an arbitrary unit that is the same throughout the whole paper. Each level  $i$  is radiatively *depopulated* at a rate  $R_i^{\text{depop}}$  equal to the sum of the rates of all transitions associated with the lines of which  $i$  is the upper level and a level  $j$  is radiatively *populated* at a rate  $R_i^{\text{pop}}$  equal to the sum of the rates of the radiative transitions populating this level, *i.e.*, those transitions for which  $j$  is the lower level:

$$R_i^{\text{depop}} = \sum_{k < i} n_{i \rightarrow k} \quad ; \quad R_i^{\text{pop}} = \sum_{k > i} n_{k \rightarrow i}.$$

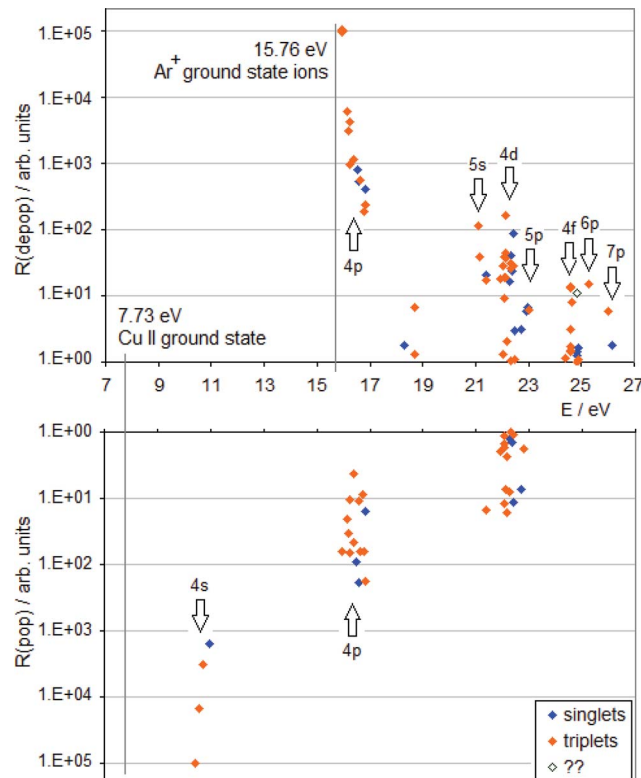


Fig. 1 TR diagram of Cu II in argon discharge ( $R(\text{pop})$  is the radiative population rate,  $R(\text{depop})$  is the radiative depopulation rate). There are no non-metastable Cu<sup>+</sup> levels below  $15.96\text{ eV}$ .

A TR diagram consists of two plots with a common abscissa scale: in the top plot, radiative *depopulation* rates ( $R^{\text{depop}}$ ) of individual levels are plotted as functions of energy, and in the bottom plot, the same is done with radiative *population* rates ( $R^{\text{pop}}$ ), except that the ordinate scale in the bottom plot has values increasing downward, see Fig. 1. The use of TR diagrams to study selective excitation processes is based on the assumption that, in glow discharges, lifetimes of upper states of most observed emission lines are largely limited by radiative decay. Then the rate of *collisional* excitation of a given state will be equal to the difference between the rate of its radiative deexcitation and the rate of its radiative excitation ( $R^{\text{col}}$ ):

$$R_i^{\text{col}} = R_i^{\text{depop}} - R_i^{\text{pop}}$$

Hence, a peak in the top plot of a TR diagram, not balanced by a peak corresponding to the same levels in the bottom plot, indicates that a collisional process is in operation, which selectively populates levels having energies in a vicinity of the peak's position. If there are high transition rates for a given level or group of levels in both plots (top and bottom), it is an indication of a cascade excitation/deexcitation sequence in which this level participates.

To complement the TR diagrams in Fig. 1 and 2, a simplified Grotrian diagram is presented in Fig. 3, showing major radiative deexcitation paths constituting the Cu II emission spectrum, along with the atomic and ionic ground and metastable states



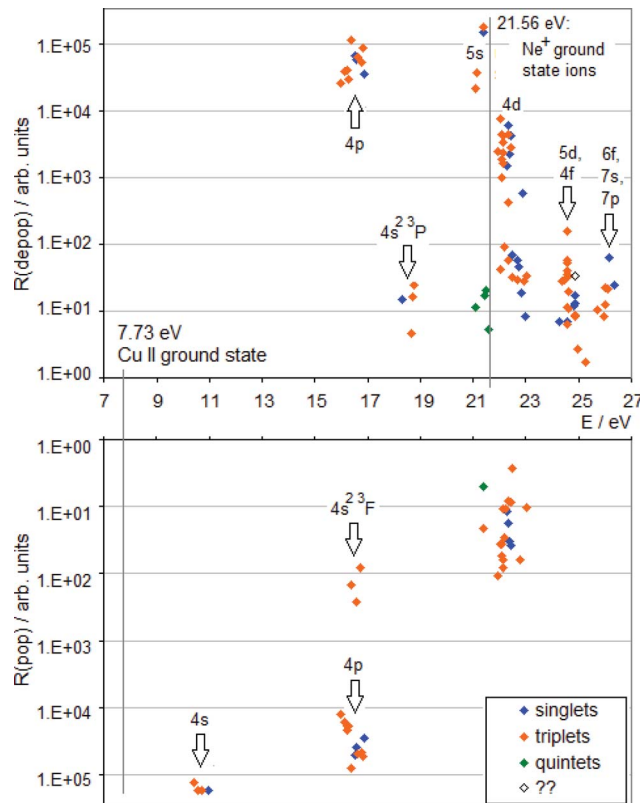


Fig. 2 TR diagram of Cu II in neon discharge ( $R(\text{pop})$ ) is the radiative population rate,  $R(\text{depop})$  is the radiative depopulation rate.

of argon and neon. The higher the transition rate observed, the thicker the line used for the corresponding transition or multiplet. Unless otherwise stated, all energies are expressed relative to the ground state of the atom. The lowest Cu II levels decaying by emission of light belong to the  $3d^9(^2D)4p$  subshell (15.96–16.85 eV) and their decay populates levels of the  $3d^9(^2D)4s$  subshell, at 10.45–10.98 eV. These levels are metastable, their decay to the Cu II ground state,  $3d^{10} \ ^1S_0$ , is both parity and angular momentum-forbidden. The difference between argon and neon discharges concerning the  $3d^9(^2D)4p$  subshell is that, in argon, the  $^3P_2$  level of this subshell is populated largely by the  $\text{Ar}^+ - \text{ACT}$  reaction, eqn (1), whilst in neon, there is a very substantial contribution of cascade excitation, affecting all the levels of this subshell, see the TR diagrams in Fig. 1 and 2. Penning ionization by neon metastables is also likely to contribute to the population of this subshell, as mentioned in,<sup>17</sup> but only an accurate quantitative analysis of radiative transition rates populating and de-populating this subshell can say how important the Penning ionization is compared to cascading. In a neon discharge, the subshell that is populated almost exclusively by  $\text{Ne}^+ - \text{ACT}$  is the  $3d^9(^2D)5s$  subshell, at 21.12–21.37 eV.

From the TR diagrams in Fig. 1 and 2, it is clear that, both in argon and neon discharges, there are many Cu II levels with energies far above the threshold for the corresponding ACT reaction between ground state copper atoms and the ions of the discharge gas used, that are significantly excited, although by 2–4 orders of magnitude less than the most strongly excited Cu

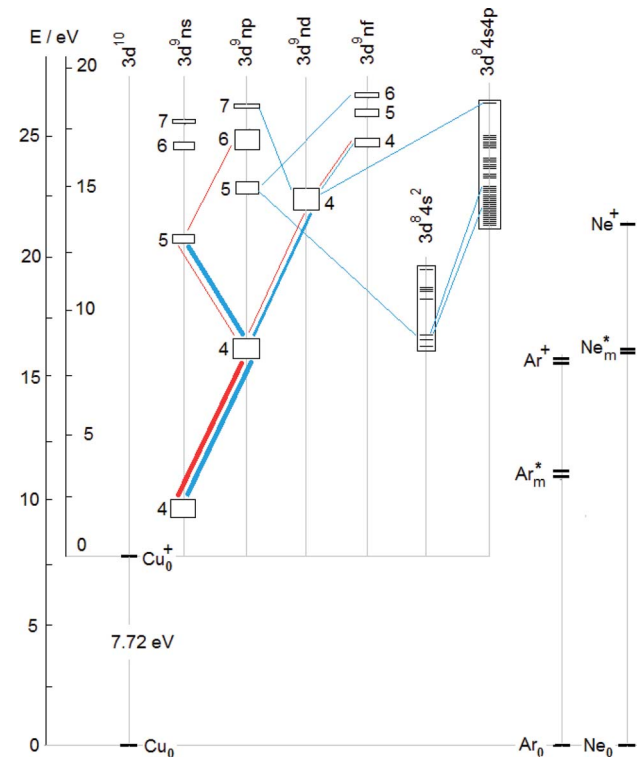
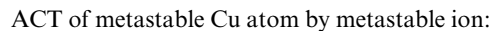
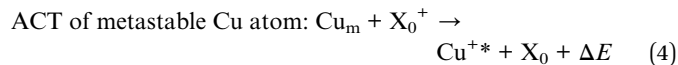
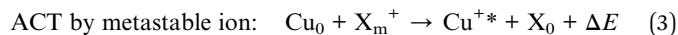
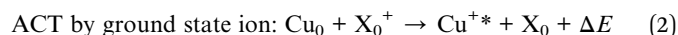
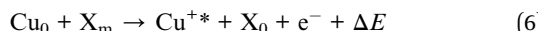


Fig. 3 Major lines and multiplets in the Cu II emission spectra in glow discharges in argon (red lines) and neon (blue lines). Left hand energy scale: total excitation energy, right hand energy scale: energy relative to the ground state of the ion.

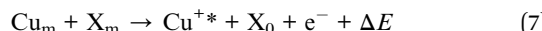
II levels. Moreover, the observed pattern of radiative deexcitation of the highest Cu II levels above ~23 eV, that are virtually unaffected by cascade processes, is different for both discharge gases. Hence, excitation mechanisms of these levels will be linked to the discharge gas used. It was suggested by Steers *et al.*<sup>3,4</sup> that some higher Cu II levels of the  $3d^9(^2D)4p$  subshell, up to the energy of ~16.85 eV, might be excited by ACT reactions between argon ions and *metastable* copper atoms with energies significantly above the Cu I ground state. But this process was then rejected by the authors as rather insignificant in the conventional unboosted dc discharge, based on comparison with a microwave-boosted discharge. The occurrence of many excited Cu II levels with high energies in the conventional dc discharge prompted us to consider in the present study the whole class of reactions, involving both ground state and metastable copper and argon atoms and ions, as possible excitation mechanisms:



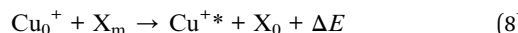
Penning ionization of ground state Cu atom:



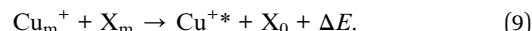
Penning ionization of metastable Cu atom:



Penning excitation of ground state Cu ion:



Penning excitation of metastable Cu ion:



Here X denotes either Ar or Ne, depending on which discharge gas is involved. Similarly to ACT, Penning *excitation*, represented by processes (8), (9), requires a good energy match. A listing of the Cu  $\pi$  subshells, the excitation of which needs to be explained, is in Table 1, together with reactions suggested to be largely responsible for their excitation. These reactions are defined in Table 2, except for reactions (10), (11), that are

**Table 1** Excitation characteristics of the  $\text{Cu}^+$  subshells the transitions from which constitute the Cu  $\pi$  emission spectrum in Ar and Ne glow discharges

$\text{Cu}^+$ subshell	$(\sum R_i^{\text{depop}})^c$		Major lines: $\lambda/\text{nm}$		Reaction Nr <sup>a</sup>		
	E/eV	In Ar	In Ne	In Ar	In Ne	In Ar	In Ne
$3d^9(^2D)4p$	15.96–16.82	$1.2 \times 10^5$	$6.5 \times 10^5$	224.700	217.941	3a, 7b, 7d	$C^b, 6a$
$3d^9(^2D)5s$	21.12–21.37	$1.9 \times 10^2$	$3.9 \times 10^5$	288.420	248.579	5b, 9a	$2a, 3b$
$3d^9(^2D)4d$	22.06–22.42	$6.4 \times 10^2$	$5.2 \times 10^4$	222.985	213.434	9a	$5a, 4a, 7c$
$3d^9(^2D)5p$	22.95–23.01	$1.2 \times 10^1$	$1.6 \times 10^2$	194.230	203.380	10a	$4a, 5a$
$3d^9(^2D_{5/2})4f$	24.57–24.62	$3.9 \times 10^1$	$4.3 \times 10^2$	510.007	518.337	10b, 11	$8a, 11$
$3d^9(^2D)5d$	24.63	$8.0 \times 10^0$	$1.6 \times 10^1$		520.511	10b, 11	$8a, 11$
$3d^9(^2D)6p$	25.28	$1.5 \times 10^1$	$1.7 \times 10^0$		317.797	10b, 11	
$3d^9(^2D_{3/2})7s$	25.94		$1.9 \times 10^1$		468.773		$4b, 11$
$3d^9(^2D)7p$	25.99–26.02	$5.7 \times 10^0$	$3.5 \times 10^1$	319.934	313.413	10b, 11	$4b, 11$
$3d^9(^2D_{5/2})6f$	26.16	$1.8 \times 10^0$	$6.3 \times 10^1$		368.655		$4b, 11$
$3d^8(^1D)4s4p(^1P^{\circ})$	26.35		$2.4 \times 10^1$		311.566		$4b, 5c, 11$

<sup>a</sup> Suggested collisional excitation process that is likely to populate this subshell (see Table 2 and the text). <sup>b</sup> Cascade excitation by radiative decay of some higher levels. <sup>c</sup> Summation over all states belonging to the given  $\text{Cu}^+$  subshell.

**Table 2** Internal energy (in eV) in possible collisions of the second kind that might result in excited  $\text{Cu}^+$  ions listed in Table 1<sup>a</sup>

	$\text{Ar}_0^+$	$\text{Ar}_m^+$	$\text{Ar}^*b$	$\text{Ne}_0^+$	$\text{Ne}_m^+$	$\text{Ne}^*c$
	$^2\text{P}^{\circ}_{3/2}$	$^2\text{P}^{\circ}_{1/2}$	$3s^23p^5(^2\text{P}^{\circ})4s$	$^2\text{P}^{\circ}_{3/2}$	$^2\text{P}^{\circ}_{1/2}$	$2s^22p^5(^2\text{P}^{\circ})3s$
E/eV	15.76	15.94	11.55–11.82	21.56	21.66	16.62–16.84
<b>Cu atoms</b>						
$3d^{10}4s\ ^2S_{1/2}$	0.00	15.94 <sup>3a</sup>		21.56 <sup>2a</sup>	21.66 <sup>3b</sup>	16.62–16.84 <sup>6a</sup>
$3d^94s^2\ ^2D$	1.39			22.95 <sup>4a</sup>	23.05 <sup>5a</sup>	
	1.64			23.20 <sup>4a</sup>		
$3d^9(^2D)4s4p(^3P^{\circ})\ ^4P^{\circ}$	4.84		16.38–16.66 <sup>7b</sup>	26.39 <sup>4b</sup>	26.49 <sup>5c</sup>	
	4.97		16.52–16.80 <sup>7b</sup>	26.53 <sup>4b</sup>		
	5.08		16.63–16.91 <sup>7b</sup>			
$3d^9(^2D)4s4p(^3P^{\circ})\ ^4F^{\circ}$	5.10		16.65–16.93 <sup>7d</sup>			
	5.15	(21.09 <sup>5b</sup> )	16.70–16.98 <sup>7d</sup>			
	5.25	21.19 <sup>5b</sup>	16.80–17.08 <sup>7d</sup>			(22.09 <sup>7c</sup> ) <sup>d</sup>
<b>Cu<sup>+</sup> ions</b>						
$3d^{10}\ ^1S_0$	7.73	23.49 <sup>10a</sup>				(24.57 <sup>8a</sup> ) <sup>d</sup>
$3d^9(^2D)4s\ ^3D$	10.45	26.21 <sup>10b</sup>	(22.28 <sup>9a</sup> ) <sup>d</sup>			
	10.56	26.32 <sup>10b</sup>	22.11–22.39 <sup>9a</sup>			
	10.70		22.25–22.53 <sup>9a</sup>			

<sup>a</sup> The superscripts are the designations of the particular reactions referred to in the last two columns of Table 1. <sup>b</sup> The same situation occurs as in the case of  $\text{Ne}^*$ , the principal quantum number n in the  $\text{Ar}^*$  level designations is higher by one. <sup>c</sup> Four  $\text{Ne}^*$  levels are in this energy interval, two of which are metastable:  $2s^22p^5(^2\text{P}^{\circ}_{3/2})3s\ ^3P_2$  and  $2s^22p^5(^2\text{P}^{\circ}_{1/2})3s\ ^3P_0$ . The other two, with  $J=1$ , are also highly populated<sup>25,26</sup> and can thus contribute to the reactions mentioned here. <sup>d</sup> Reaction with argon atom in the  $3s^23p^5(^2\text{P}^{\circ}_{1/2})4s\ ^3P_1$  state or with neon atom in the  $2s^22p^5(^2\text{P}^{\circ}_{1/2})3s\ ^3P_1$  state.

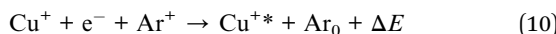


defined in the text below. In Table 2, the copper ground state and metastable atoms and ions entering the suggested reactions (the first column) are combined with the species related to the discharge gas (the first row) and for each pair of the initial reactants considered, their total internal energy is given in the corresponding cell. Individual reactions are shown in the last two columns of Table 1 and denoted in Table 2 by superscripts attached to the internal energy involved. Each entry consists of a number, specifying the type of the reaction (the number of the corresponding equation above), combined with a letter which defines the reaction unambiguously, *i.e.*, is specific for the given pair of reacting species. These species are specified in the header of the column and in the first cell of the row to which the cell showing that reaction belongs. For example, the ACT reaction mentioned in Section 1 and described by eqn (1), responsible for excitation of the 224.700 nm line, is a special case of the process described by eqn (3) and in Table 2 it has the designation '3a'. Similarly, reaction '3b' is the following:

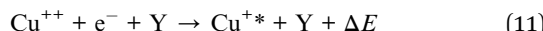


Reactions between reactants differing only in a particular level involved, but belonging to the same term, are classified as identical, *i.e.*, have the same designation (the same superscript) in Tables 1 and 2. Tables 1 and 2 do not contain collisional processes that are not reflected in the Cu II emission spectrum, such as *e.g.* the creation of the Cu<sup>+</sup> ground state and 3d<sup>9</sup>(<sup>2</sup>D)4s metastable ions in an argon discharge by Penning ionization. Also electron impact excitation/ionization is not discussed. Such processes must be accounted for in any complete collisional-radiative models of copper ions in these glow discharges.

What remains to be discussed are the reactions '10a', '10b' and '11'. In an argon discharge, some Cu II states with energies greater than ~24 eV are also excited. Such energies are not linked to any reaction mentioned so far. It may be worth to consider the following reaction:



in which a low energy electron in between a Cu<sup>+</sup> and an Ar<sup>+</sup> ions on a collision trajectory would diminish their electrostatic repulsion and they might form a loosely-bound temporary molecular ion, the decay of which could yield the copper ion excited to the very high energy required. An alternative process would be the neutralisation of Cu<sup>++</sup> ions,



where Y is a third body (three-body recombination<sup>24</sup>). Further work is being carried out to distinguish between these hypotheses for the excitation in argon discharge of the Cu II levels with energies around 25 eV.

### 3. Summary and conclusions

The Cu II emission spectra observed in analytical glow discharges in argon and neon with a copper cathode were used to calculate transition rate diagrams of copper ions in these

discharges. Based on the TR diagrams, the Cu II levels excited were identified and 16 different collisional processes ((7) in argon and (9) in neon) between ground state- and metastable atoms and ions of copper and the discharge gas were proposed as probably significant for populating those Cu II levels. These processes can explain the observed Cu II spectra to a large extent.

### References

- Y. Zhao and G. Horlick, Emission spectral characteristics of Cu, Ag, Zn and Cd neutral atoms in a glow discharge, *Spectrochim. Acta, Part B*, 2006, **61**, 674–685.
- Y. Zhao and G. Horlick, A spectral study of charge transfer and Penning processes for Cu, Zn, Ag and Cd in a glow discharge, *Spectrochim. Acta, Part B*, 2006, **61**, 660–673.
- E. B. M. Steers and R. J. Fielding, Charge-transfer excitation processes in the Grimm lamp, *J. Anal. At. Spectrom.*, 1987, **2**, 239–244.
- E. B. M. Steers and F. Leis, Observations on the use of the microwave-boosted glow discharge lamp and relevant excitation processes, *J. Anal. At. Spectrom.*, 1989, **4**, 199–204.
- E. B. M. Steers and F. Leis, Excitation of the spectra of neutral and singly ionized atoms in the Grimm-type discharge lamp, with and without supplementary microwave excitation, *Spectrochim. Acta, Part B*, 1991, **46**, 527–537.
- E. B. M. Steers, Charge transfer excitation in glow discharge sources: the spectra of titanium and copper with neon, argon and krypton as plasma gas, *J. Anal. At. Spectrom.*, 1997, **12**, 1033–1040.
- K. Wagatsuma and K. Hirokawa, Spectrometric studies of excitation mechanisms on singly-ionized copper emission lines in Grimm-type glow discharge plasmas with helium mixture technique, *Spectrochim. Acta, Part B*, 1991, **46**, 269–281.
- K. Wagatsuma and K. Hirokawa, Observation of singly-ionized copper emission lines from a Grimm-type glow discharge plasma with argon–helium gas mixtures in a visible wavelength region, *Spectrochim. Acta, Part B*, 1993, **46**, 1039–1044.
- A. Bogaerts and R. Gijbels, Comparison of argon and neon as discharge gases in a direct-current glow discharge: a mathematical simulation, *Spectrochim. Acta, Part B*, 1997, **52**, 553–565.
- A. Bogaerts and R. Gijbels, Collisional-radiative model for the sputtered copper atoms and ions in a direct current argon glow discharge, *Spectrochim. Acta, Part B*, 1998, **53**, 1679–1703.
- A. Bogaerts, Z. Donko, K. Kutasi, G. Bano, N. Pinhao and M. Pinheiro, Comparison of calculated and measured optical emission intensities in a direct current argon–copper glow discharge, *Spectrochim. Acta, Part B*, 2000, **55**, 1465–1479.
- V.-D. Hodoroaba, V. Hoffmann, E. B. M. Steers and K. Wetzig, Emission spectra of copper and argon in an argon glow discharge containing small quantities of hydrogen, *J. Anal. At. Spectrom.*, 2000, **15**, 951–958.



13 V.-D. Hodoroaba, E. B. M. Steers, V. Hoffmann and K. Wetzig, The effect of small quantities of hydrogen on a glow discharge in neon. Comparison with the argon case, *J. Anal. At. Spectrom.*, 2001, **16**, 43–49.

14 S. Mushtaq, E. B. M. Steers, J. C. Pickering and V. Weinstein, Asymmetric charge transfer involving the ions of added gases (oxygen or hydrogen) in Grimm-type glow discharges in argon or neon, *J. Anal. At. Spectrom.*, 2012, **27**, 1263–1273.

15 Z. Weiss, Glow discharge excitation and matrix effects in the Zn–Al–Cu system in argon and neon, *Spectrochim. Acta, Part B*, 2007, **62**, 787–798.

16 S. Mushtaq, E. B. M. Steers, J. C. Pickering and K. Putyera, Selective and non-selective excitation/ionization processes in analytical glow discharges: excitation of the ionic spectra in argon/helium mixed plasmas, *J. Anal. At. Spectrom.*, 2014, **29**, 681–695.

17 S. Mushtaq, E. B. M. Steers, J. C. Pickering and W. Weinstein, Effect of small quantities of oxygen in a neon glow discharge, *J. Anal. At. Spectrom.*, 2014, **29**, 2027–2041.

18 K. Rózsa, P. Mezei, M. Janossy, F. Howarka and J. Kuen, Endoergic charge transfer reactions in the cathode glow, Proceedings of Symp. on At. and Surf. Physics (SASP), Obertraun, Austria, 1986, pp. 263–267.

19 P. Mezei, K. Rózsa, M. Janossy and P. Apai, Endoergic and resonant charge transfer excitation in He–Cu discharge, *J. Phys. D: Appl. Phys.*, 1987, **34**, 71–74.

20 Z. Weiss, E. B. M. Steers, J. C. Pickering and S. Mushtaq, Transition rate diagrams – A new approach to the study of selective excitation processes: The spectrum of manganese in a Grimm-type glow discharge, *Spectrochim. Acta, Part B*, 2014, **92**, 70–83.

21 Z. Weiss, E. B. M. Steers, J. C. Pickering and S. Mushtaq, Excitation and transition rate diagrams of singly ionized iron in analytical glow discharges in argon, neon and argon–hydrogen mixture, *J. Anal. At. Spectrom.*, 2014, **29**, 2078–2090.

22 J. C. Pickering, High resolution Fourier transform spectroscopy with the Imperial College (IC) UV-FT spectrometer, and its applications to astrophysics and atmospheric physics: a review, *Vib. Spectrosc.*, 2002, **29**, 27–43.

23 S. Mushtaq, V. Hoffmann, E. B. M. Steers and J. C. Pickering, Comparison of a sample containing oxide with a pure sample with argon–oxygen mixtures, *J. Anal. At. Spectrom.*, 2012, **27**, 1423–1431.

24 B. Chapman, *Glow Discharge Processes*, J. Wiley, 1980.

25 C. E. Light, A study of spectral line intensities and excited atom populations in a hollow cathode discharge, PhD thesis, Council for National Academic Awards, 1989.

26 R. Djulgerova, D. Jechev, Y. Pacheva and S. Rashev, On the population of neon levels in the low temperature plasma of a hollow cathode discharge, *Spectrosc. Lett.*, 1975, **8**, 1001–1008.

